nature communications

Article

https://doi.org/10.1038/s41467-025-59664-8

Direct evaluation of antiplatelet therapy in coronary artery disease by comprehensive image-based profiling of circulating platelets

Received: 14 March 2024

Accepted: 29 April 2025

Published online: 15 May 2025

Check for updates

Kazutoshi Hirose[1], Satoshi Kodera[1], Masako Nishikawa[2] ✉, Masataka Sato[1], Yuqi Zhou[3], Hongqian Zhang[3], Shun Minatsuki[1], Junichi Ishida[1], Norifumi Takeda[1], Huidong Wang[3], Chuiming Kong[3], Yunjie Deng[3], Junyu Chen[3], Chenqi Zhang[3], Jun Akita[3], Yuma Ibayashi[3], Ruoxi Yang[3], Hiroshi Kanno[3,4], Nao Nitta[5], Takeaki Sugimura[5], Norihiko Takeda[1], Makoto Kurano[2], Yutaka Yatomi[2,6] & Keisuke Goda[3,5,7,8,9] ✉

Coronary artery disease (CAD) is a leading cause of death globally. Antiplatelet therapy remains crucial in preventing and treating CAD-associated thrombotic complications, but it concurrently amplifies the risk of bleeding. Unfortunately, traditional platelet function measurement methods cannot directly evaluate its efficacy and safety. Here we demonstrate comprehensive image-based profiling of circulating platelets to directly observe thrombotic conditions and assess antiplatelet therapy in CAD patients. Deep learning-based analysis of whole blood samples from 207 CAD patients revealed elevated concentrations of circulating platelet aggregates, especially in acute versus chronic coronary syndrome patients. It also indicated a regimen-dependent reduction in these concentrations upon treatment with antiplatelet drugs, thereby verifying the direct efficacy of the therapy. Notably, consistent concentrations of these aggregates were found in both venous and arterial blood, suggesting venous blood as a reliable therapy efficacy indicator, despite CAD's arterial nature. These findings support personalized and improved antiplatelet therapy in CAD management.

Coronary artery disease (CAD) is a significant health challenge worldwide, affecting over 200 million people and resulting in about 10 million deaths each year[1]. Histological studies have identified increased platelet aggregation and subsequent thrombus formation as key factors in the pathogenesis of CAD, encompassing both acute coronary syndrome (ACS) and chronic coronary syndrome (CCS)[2–6]. While recent progress in CAD management has improved patient outcomes and reduced symptoms[7–9], the cornerstone of thrombotic event prevention and treatment in post-revascularization scenarios heavily relies on antiplatelet therapy, primarily through the administration of aspirin and $P2Y_{12}$ receptor inhibitors[10–12]. Despite its clear benefits, this therapy concurrently amplifies the risk of bleeding, potentially increasing mortality rates 3-fold to 5-fold[13,14]. Hence, individualized assessment of the effects of antiplatelet drugs on platelet

[1]Department of Cardiovascular Medicine, The University of Tokyo, Tokyo, Japan. [2]Department of Clinical Laboratory Medicine, The University of Tokyo, Tokyo, Japan. [3]Department of Chemistry, The University of Tokyo, Tokyo, Japan. [4]Department of Neurosurgical Engineering and Translational Neuroscience, Tohoku University Graduate School of Medicine, Miyagi, Japan. [5]CYBO Inc, Tokyo, Japan. [6]International University of Health and Welfare Graduate School, Tokyo, Japan. [7]Department of Bioengineering, University of California, Los Angeles, CA, USA. [8]Institute of Technological Sciences, Wuhan University, Hubei, China. [9]International Center for Synchrotron Radiation Innovation Smart (SRIS), Tohoku University, Miyagi, Japan. ✉e-mail: msknishikawa-tky@umin.ac.jp; goda@chem.s.u-tokyo.ac.jp

aggregation is vital to strike a balance between their efficacy and safety.

Unfortunately, traditional methods for measuring platelet function fall short of addressing the full spectrum of clinical needs. A range of techniques have been explored, including clinical laboratory-based methods such as light transmission aggregometry, impedance aggregometry, and flow-cytometric analysis of vasodilator-stimulated phosphoprotein, along with point-of-care assays such as VerifyNow and Multiplate[15–18]. However, a major limitation of these methods is their indirect nature in assessing platelet responses to specific antiplatelet agents (Supplementary Table 1)[16,19,20]. Furthermore, these methods generally do not replicate the complex in vivo conditions under which platelets operate within the human body[21,22]. Critical factors such as blood flow dynamics, interactions with vascular endothelium, and the presence of other blood cells significantly influence platelet behavior[15,19,23]. In vitro tests can fail to capture these critical aspects, potentially leading to discrepancies between the test results and the actual platelet function in the patient's body.

In this work, we build on our recent development of a comprehensive image-based profiling method for circulating platelets[24] to directly observe thrombotic conditions and assess the effectiveness of antiplatelet treatment in CAD patients. Specifically, as shown in Fig. 1, our data-driven study follows four steps: (i) collecting a 1 mL blood sample from each of 207 CAD patients (Supplementary Table 2, Source Data); (ii) isolating platelet-related objects, including single platelets, platelet-platelet aggregates, and platelet-leukocyte aggregates (Supplementary Fig. 1); (iii) high-throughput, blur-free, bright-field imaging of the objects; and (iv) performing digital image analysis including deep learning-based phenotypic classification and statistical analysis of the objects in the acquired images. Deep learning-based analysis of whole blood samples from the 207 CAD patients revealed elevated concentrations of circulating platelet aggregates, particularly in ACS versus CCS patients. Furthermore, a regimen-dependent reduction in these aggregates was observed following antiplatelet therapy, confirming its direct efficacy. Notably, similar aggregate concentrations were detected in both venous and arterial blood, indicating that venous blood, despite CAD's arterial nature, may serve as a reliable indicator of therapy efficacy. These findings support personalized and improved antiplatelet therapy for CAD management.

Results

Baseline characteristics, peri-procedural antithrombotic treatment, and procedural strategies

Supplementary Table 2 displays baseline characteristics, including risk factors, medical history, and laboratory parameters for the 207 CAD patients (81.6% male). The average age was 72 ± 11 years. Among the patients, 42 (20.3%) presented with ACS, and 88 (42.5%) had a history of coronary artery revascularization, including 76 (36.7%) with percutaneous coronary intervention (PCI) alone, 6 (2.9%) with coronary artery bypass grafting (CABG) alone, and 6 (2.9%) with a combination of PCI and CABG. Upon admission, 169 (81.6%) patients were prescribed antithrombotic drugs. Angiographic findings, presented in Supplementary Table 2, reveal that 131 (63.3%) patients had multivessel disease.

Details of peri-procedural antithrombotic treatment are provided in Supplementary Table 3. Briefly, 197 patients (95.2%) received antithrombotic drugs prior to coronary angiography (CAG) or PCI, with 62 patients (30.0%) on monotherapy, 124 (59.9%) on dual therapy, and 11 (5.3%) on triple therapy. Among them, 193 patients (93.2%) were prescribed antiplatelet medications, including 76 (36.7%) on single antiplatelet therapy (SAPT) and 117 (56.5%) on dual antiplatelet therapy (DAPT), while 34 patients (16.4%) were on anticoagulant therapy.

Procedural strategies are summarized in Supplementary Table 4. Of the 144 patients who underwent PCI, stents were implanted in 114 (79.2%), with 90 treated with a single stent. Drug-coated balloons were used in 38 patients (26.4%), and debulking techniques (rotational/orbital atherectomy or intravascular lithotripsy) in 24 patients (16.7%). Intravascular imaging was employed in all patients, revealing vulnerable plaques in 34 (23.6%), thrombi in 19 (13.2%), and heavily calcified plaques (over 180 degrees) in 62 (43.1%) patients.

Comprehensive image acquisition

We applied an optical frequency-division-multiplexed (FDM) microscope previously developed by ourselves[24–26] to acquire high-

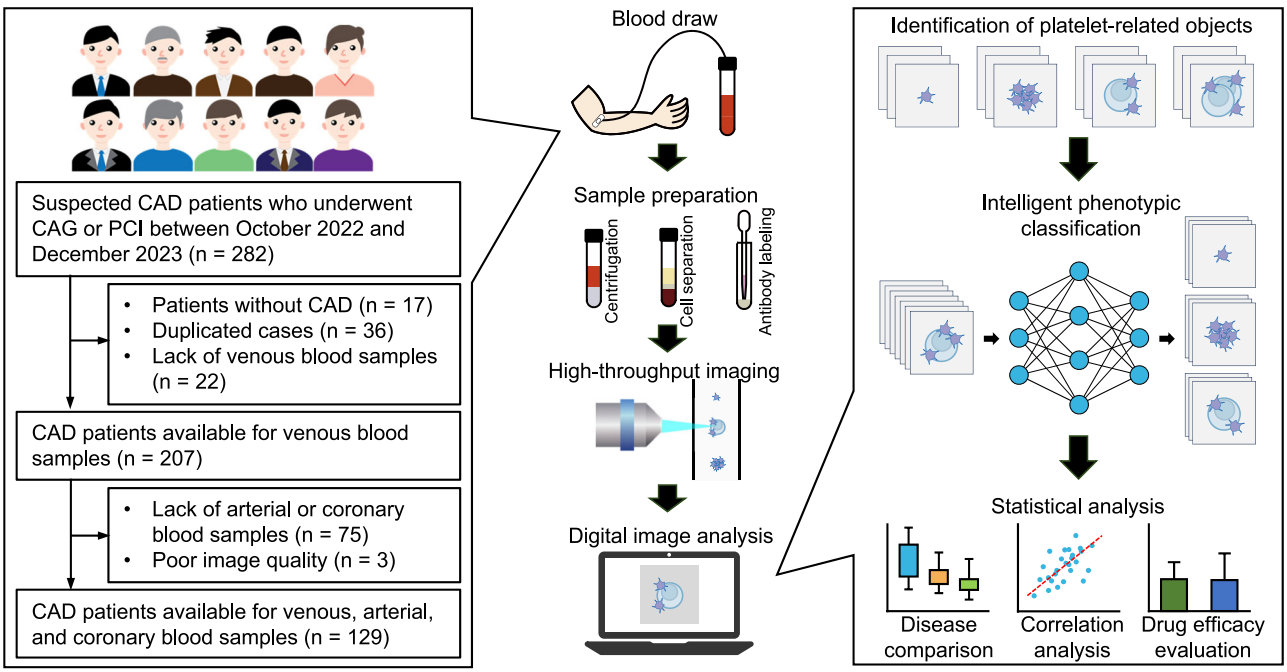

Fig. 1 | Comprehensive image-based profiling of circulating platelets. The experimental workflow consists of blood draw, sample preparation, high-throughput imaging, and digital image analysis. Insets show the study flow chart and the details of the digital image analysis. CAD coronary artery disease, CAG coronary angiography, PCI percutaneous coronary intervention.

https://doi.org/10.1038/s41467-025-59664-8

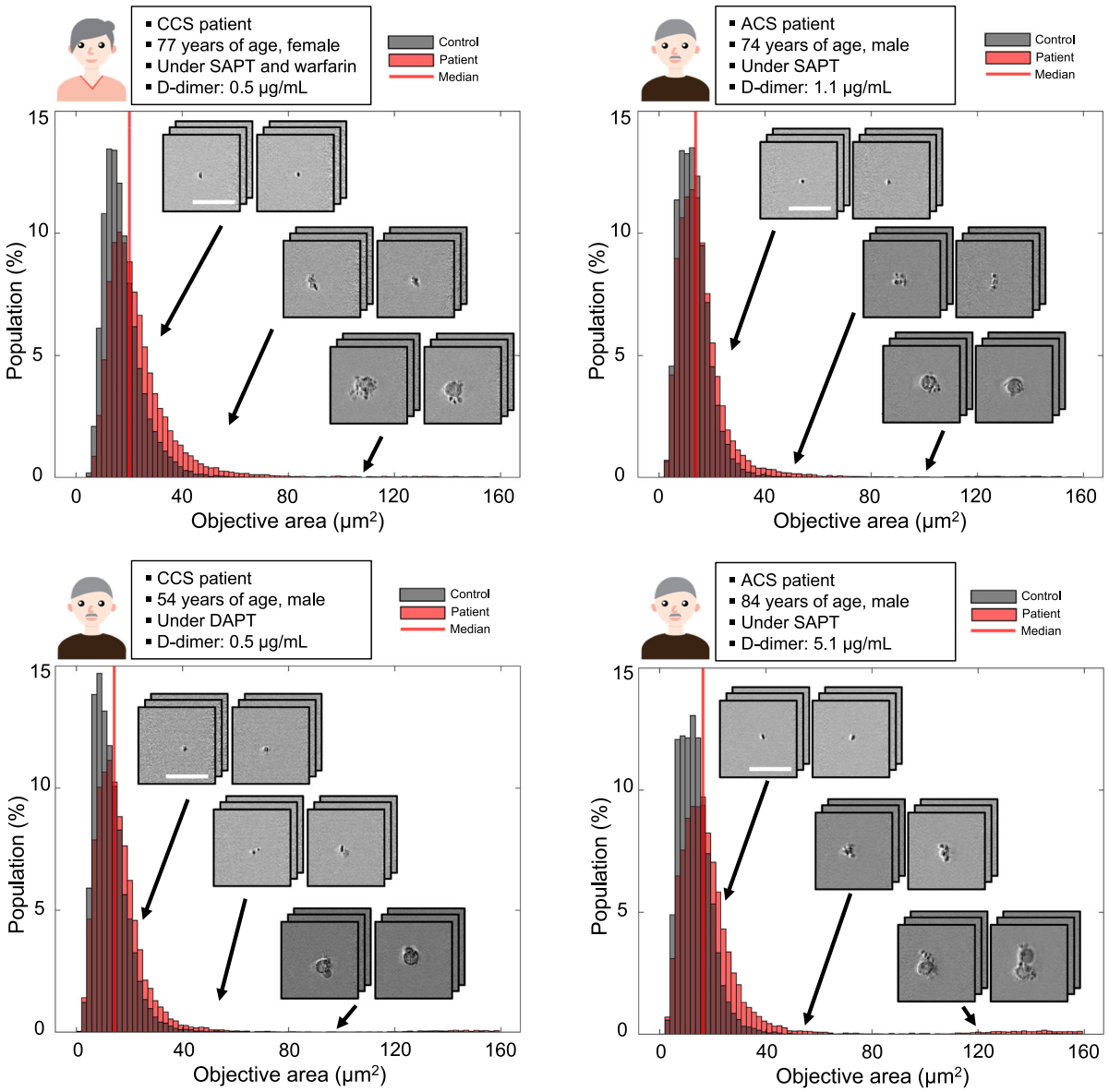

Fig. 2 | Representative histograms of platelet-related objects in CAD patients. The objective area is defined as the area of a platelet-related object (i.e., a single platelet, a platelet-platelet aggregate, or a platelet-leukocyte aggregate) in each image. Each histogram comprises 25,000 images of platelet-related objects. Insets show the representative images of platelet-related objects. ACS acute coronary syndrome, CCS chronic coronary syndrome, SAPT single antiplatelet therapy, DAPT dual antiplatelet therapy. Source data are provided as a Source Data file.

throughput, blur-free, bright-field images of circulating platelets flowing rapidly at 1 m/s on a hydrodynamic-focusing microfluidic chip (Supplementary Fig. 2a, Methods). The FDM microscope was specifically triggered by fluorescence signals from anti-CD61-PE-labeled platelets to capture images of platelet-related objects, thereby enhancing focus on relevant events while avoiding its throughput from being consumed by non-platelet events (see Methods for further details). Figure 2 shows the typical histograms for the bright-field images (67 × 67 pixels per image) of circulating single platelets and platelet aggregates. These images were captured over a field of view of 53.6 × 53.6 μm² with a spatial resolution of 0.8 μm (Supplementary Fig. 2b). For each imaging run (sample), 25,000 images were acquired with the event rate ranging from 100 to 300 events per second (eps), where an event is identified as a single platelet, a platelet aggregate, or a piece of cellular debris containing one or more platelets. Residual components such as erythrocytes, leukocytes excluding those contained in platelet-leukocyte aggregates, and cellular debris were ignored and not detected as events. The event rate was chosen to avoid clogging the microchannel in the microfluidic chip, although the theoretical event rate of the FDM microscope was over 10,000 eps.

Intelligent phenotypic classification

We developed a deep convolutional neural network (CNN) model trained via AIDeveloper (v. 0.2.3)[27] to perform deep learning-based phenotypic classification of all objects in all patient and control samples (Supplementary Fig. 3a, b, "Methods"). Firstly, object recognition based on an efficient contour detection algorithm was performed on 25,000 images using OpenCV[28,29]. All blank images where no objects were detected were removed. The remaining images were fed into the CNN model and classified into seven categories: (i) noise, (ii) a single platelet, (iii) a platelet-platelet aggregate, (iv) a platelet aggregate composed of a single leukocyte and a single platelet, (v) a platelet aggregate composed of a single leukocyte and multiple platelets, (vi) a platelet aggregate composed of multiple leukocytes and a single platelet, and (vii) a platelet aggregate composed of multiple leukocytes

https://doi.org/10.1038/s41467-025-59664-8

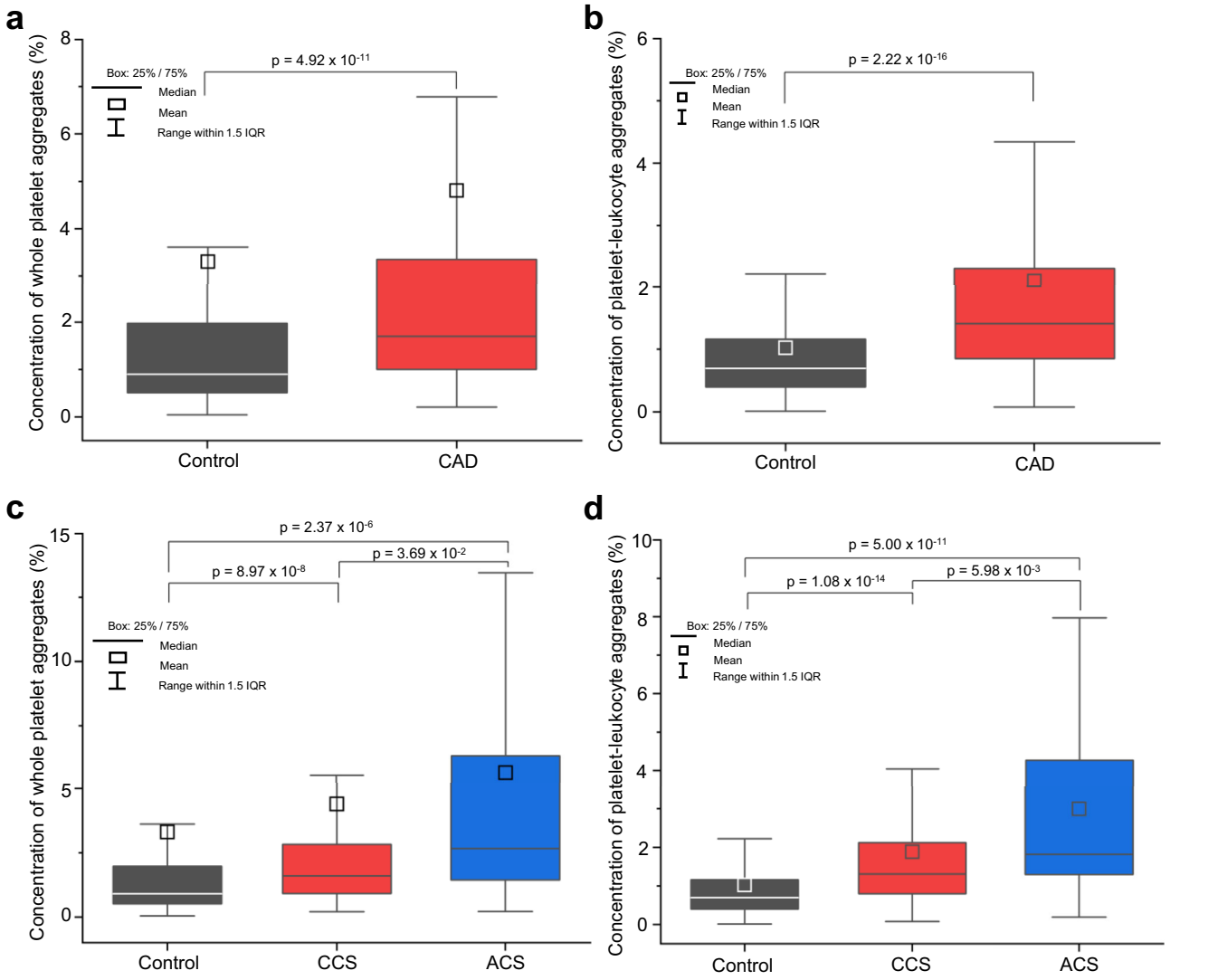

Fig. 3 | Increased in vivo platelet aggregation observed in CAD patients. *P* values of each pair of adjacent classes were obtained using the two-sided Steel-Dwass test and are shown in the figure. **a**, **b** Comparison of the concentrations of circulating whole platelet aggregates and platelet-leukocyte aggregates between CAD patients ($n = 207$) and healthy subjects. **c**, **d** Comparison of the concentrations of circulating whole platelet aggregates and platelet-leukocyte aggregates between ACS patients ($n = 42$), CCS patients ($n = 165$), and healthy subjects. $p = 1.13 \times 10^{-10}$ (**c**) and 5.38×10^{-20} (**d**) with the Kruskal–Wallis test. CAD coronary artery disease, ACS acute coronary syndrome, CCS chronic coronary syndrome. Source data are provided as a Source Data file.

and multiple platelets. The category of (i) noise was defined as images containing other less critical components, such as residual erythrocytes, leukocytes, and cellular debris. Categories (iv) – (vii) were divided to improve model accuracy and were all considered as platelet-leukocyte aggregates. The CNN model achieved a confusion matrix with classes (i), (ii), (iii), and (iv)–(vii) combined, reaching an average accuracy of 96.4% (Supplementary Fig. 3c, d). The concentration of circulating whole platelet aggregates was defined as the ratio of the number of images containing objects with an area exceeding 48 μm^2 (the threshold value beyond which single platelets were absent in control samples)[24] in each image to the total number of non-blank images across categories (ii) to (vii), which is roughly equal to the total number of non-blank images in category (ii), reflecting the predominance of platelets (150,000–450,000 platelets/μL of blood) over leukocytes (4000–11,000 leukocytes/μL of blood) in blood. Similarly, the concentration of circulating platelet-leukocyte aggregates was defined as the ratio of the number of images in categories (iv) to (vii) to the total number of non-blank images in categories (ii) – (vii), which is nearly equivalent to the total number of non-blank images in category (ii).

Comparing in vivo platelet aggregation levels between CAD patients and healthy subjects

We conducted a comparative analysis of the concentration of circulating platelet aggregates in 248 venous blood samples from 207 CAD patients against 128 venous samples from 12 healthy individuals (control group), ensuring identical conditions for sample preparation and image acquisition on the same day. Despite 86.5% of the patients undergoing antithrombotic therapy, they displayed elevated platelet aggregate concentrations compared to the healthy subjects ($p < 0.001$; Fig. 3a). This discrepancy was also confirmed for platelet-leukocyte aggregates, including platelet-monocyte aggregates ($p < 0.001$; Fig. 3b), likely because activated platelets have a higher tendency to bind to monocytes, making platelet-monocyte aggregates a sensitive marker for in vivo platelet activation[30,31]. These findings are consistent with previous research[31,32], demonstrating significantly enhanced precision by virtue of the CNN-based phenotypic classification in this study. Moreover, when segregating CAD patients into ACS and CCS groups receiving similar types of P2Y12 inhibitors (clopidogrel or prasugrel), both groups continued to show higher platelet aggregate concentrations compared to the control group (both $p < 0.001$) and

more pronounced platelet aggregation in ACS than CCS ($p = 0.037$ Fig. 3c). The consistent associations were shown regarding the platelet-leukocyte aggregates ($p < 0.001$ for both ACS and CCS vs control, $p = 0.006$ for ACS vs CCS; Fig. 3d). A sensitivity analysis, excluding patients with intermediate stenosis who had no prior coronary revascularization ($n = 4$), confirmed consistent associations between CAD patients and healthy subjects, as well as among ACS, CCS, and control groups.

Analyzing antiplatelet therapy's effect on in vivo platelet aggregation in CAD patients

We explored the correlation between different antithrombotic regimens and the concentration of platelet aggregates using venous blood samples, with the details of the antithrombotic therapy provided in Supplementary Table 3. At the time of blood collection, 179 (86.5%) patients were receiving some form of antithrombotic treatment: 68 (32.9%) were on monotherapy, 104 (50.2%) on dual therapy, and 7 (3.4%) on triple therapy. Of these patients, 169 (81.6%) were prescribed antiplatelet medications, including 73 (35.3%) on SAPT and 96 (46.4%) on DAPT. Additionally, 32 (15.5%) patients were on anticoagulant medications (Supplementary Table 3). Our analysis showed a significant decrease in the concentrations of whole platelet aggregates and platelet-leukocyte aggregates in CAD patients treated with multiple (≥2) antithrombotic drugs, in comparison to those without any antithrombotic therapy ($p < 0.001$ in the whole platelet aggregates and $p = 0.003$ in the platelet-leukocyte aggregates) and those on monotherapy ($p = 0.023$ in the whole platelet aggregates and $p = 0.254$ in the platelet-leukocyte aggregates; Fig. 4a, b). When examining antiplatelet therapy more closely, we found that both the SAPT and DAPT groups exhibited a significant reduction in the concentration of whole platelet aggregates compared to patients not receiving antiplatelet therapy (both $p < 0.05$). However, there was no significant difference in whole platelet aggregate and platelet-leukocyte aggregate concentrations between the SAPT and DAPT groups ($p < 0.3$; Fig. 4c, d). A sensitivity analysis, which excluded patients on anticoagulant therapy, revealed a significant reduction in the concentration of whole platelet aggregates within the DAPT ($p < 0.001$) group and in the concentration of platelet-leukocyte aggregates within the DAPT group ($p = 0.002$), although there was no significant difference in these concentrations between the SAPT and DAPT groups (Fig. 4e, f). Finally, we performed a sensitivity analysis of 203 CAD patients with significant stenosis or a history of coronary revascularization showed consistent results with the overall study population.

Comparing in vivo platelet aggregation levels across different blood sampling sites in CAD patients

In an analysis of 129 CAD patients with blood samples taken from both peripheral and coronary arteries, we examined the relationship between the site of blood sampling and the concentration of platelet aggregates (see Supplementary Tables 5–7 for their baseline and procedural characteristics, pharmacological therapy, and procedural outcomes). Our findings indicate no significant difference in platelet aggregate concentration between venous, peripheral arterial, and coronary arterial blood. Intriguingly, while the activated clotting time (ACT), a measure of unfractionated heparin (UFH) efficacy, was considerably longer in the coronary artery than in peripheral arteries [196 (161–289) seconds vs. 112 (102–147) seconds, $p < 0.001$], this extended clotting time did not correspond to a difference in platelet aggregate concentration between these arterial sites. Notably, there was a strong correlation between platelet aggregate concentrations in peripheral and coronary arteries ($r = 0.91$, $p < 0.001$; Fig. 5a). Venous samples showed a moderate correlation with both peripheral ($r = 0.76$, $p < 0.001$; Fig. 5b) and coronary arterial samples ($r = 0.76$, $p < 0.001$; Fig. 5c). Furthermore, we conducted an exploratory analysis on 36 patients who had their venous blood sampled on the same day as CAG or PCI. This subset demonstrated a similar relationship between the peripheral and coronary arteries ($r = 0.89$, $p < 0.001$; Fig. 5d), and even stronger correlations between the vein and peripheral artery ($r = 0.86$, $p < 0.001$; Fig. 5e) and between the vein and coronary artery ($r = 0.86$, $p < 0.001$; Fig. 5f). In addition, we compared the concentrations of platelet-leukocyte aggregates among venous, peripheral and coronary arterial blood samples, displaying moderate associations between the peripheral and coronary arteries ($r = 0.75$, $p < 0.001$), the vein and peripheral artery ($r = 0.44$, $p < 0.001$), and the vein and coronary artery ($r = 0.43$, $p < 0.001$). Further analysis on patients receiving blood sampling on the day of catheterization also revealed similar correlations of platelet-leukocyte aggregate concentrations than whole platelet aggregates; $r = 0.74$, $p < 0.001$ in the peripheral and coronary arteries; $r = 0.53$, $p < 0.001$ in the vein and peripheral artery; $r = 0.56$, $p < 0.001$ in the vein and coronary artery (Supplementary Fig. 4a–c). An extensive analysis of 127 patients with significant stenosis or a history of coronary artery revascularization also confirmed the strong correlations in these concentrations between venous and arterial sampling sites. These findings indicate that venous blood can reflect the state of platelet aggregation in both coronary and peripheral arteries in vivo on the day of blood collection. They also suggest that venous blood may serve as a reliable marker for the effectiveness of antiplatelet therapy in CAD patients, despite the primarily arterial nature of the disease. This insight could have significant implications for non-invasive monitoring and managing CAD.

Longitudinal assessment of antiplatelet therapy's effect on in vivo platelet aggregation in CAD patients

We observed the temporal effect of antiplatelet therapy on the concentrations of circulating whole platelet aggregates in 32 CAD patients who underwent multiple procedures during the study period. For instance, Patient 1, diagnosed with CCS and treated with SAPT (aspirin) before an initial CAG procedure, exhibited a reduced level of whole platelet aggregates in a venous sample after switching to DAPT (aspirin and clopidogrel), which was maintained through the first and second PCI procedures (Fig. 6a). Patient 2, also with CCS, was on SAPT (aspirin) during a CAG procedure and moved to DAPT (aspirin and prasugrel) for a subsequent PCI procedure involving drug-eluting stents. This patient's whole platelet aggregate concentration decreased after the procedure, with a further reduction observed after the second PCI (Fig. 6b). Moreover, Patients 3 and 4, both diagnosed with ACS and initially treated with SAPT (aspirin), underwent emergency PCI and started on DAPT (aspirin and prasugrel) during the procedure, showing significant reductions in circulating whole platelet aggregate concentrations following the upgrade in antiplatelet therapy (Fig. 6c, d). Variations in baseline whole platelet aggregate concentrations across these cases may be linked to underlying conditions (chronic lymphocytic leukemia without disease progression in Patient 1 and a prolonged history of CAD marked by multiple prior PCI procedures and chronically completely occluded lesions aside from the culprit lesion in Patient 4). The slight fluctuations in whole platelet aggregate levels observed are likely due to individual differences and the inherent variability among patients[33].

Discussion

This study yielded three significant findings: (1) Patients with CAD, particularly those with ACS versus CCS, exhibited increased concentrations of circulating whole platelet aggregates and platelet-leukocyte aggregates in peripheral veins compared to healthy subjects; (2) The concentrations of circulating whole platelet aggregates and platelet-leukocyte aggregates significantly diminished in

https://doi.org/10.1038/s41467-025-59664-8

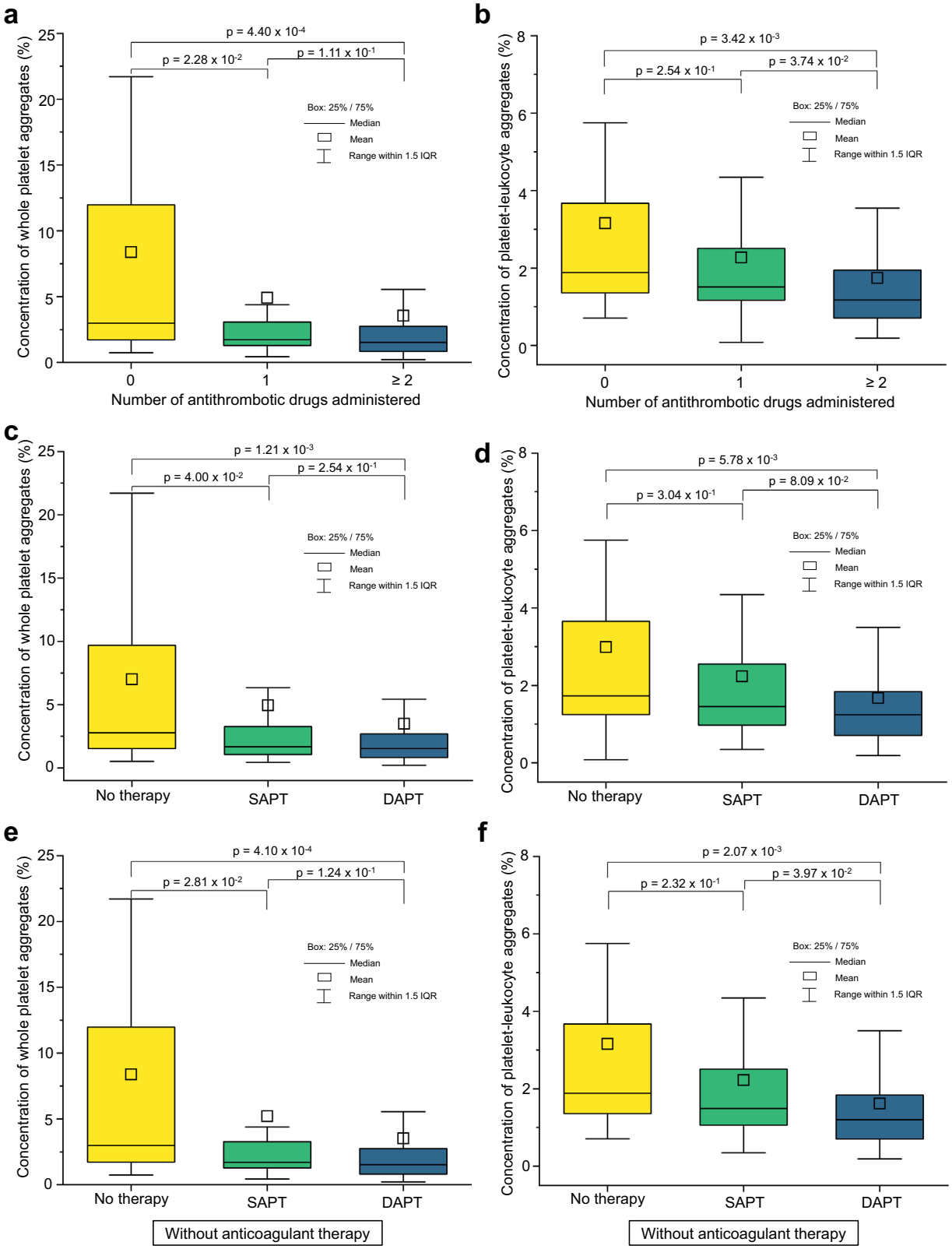

CAD patients undergoing antiplatelet therapy, whereas they remained similar between those receiving and not receiving anticoagulant drugs; (3) The concentrations of circulating whole platelet aggregates and platelet-leukocyte aggregates in peripheral veins closely mirrored those in both peripheral and coronary arteries, despite CAD's arterial nature. These insights were enabled by the FDM microscope and deep learning-based phenotypic classification, allowing for the direct assessment of thrombotic conditions and the efficacy of antiplatelet therapy in CAD. These findings offer a promising pathway to personalized and improved antiplatelet therapy in CAD management.

It is well-established histologically that heightened platelet aggregation, leading to thrombus formation, is a primary factor in the progression of CAD, including ACS and CCS[2–6]. Despite the critical role

Fig. 4 | Reduced in vivo platelet aggregation observed in CAD patients following antiplatelet therapy. *P* values of each pair of adjacent classes were obtained using the two-sided Steel-Dwass test and are shown in the figure. **a**, **b** Effect of antithrombotic therapy on the concentrations of circulating whole platelet aggregates and platelet-leukocyte aggregates in CAD patients (n = 28 for no drug, $n = 68$ for one drug administered, $n = 111$ for two or more drugs administered). $p = 2.82 \times 10^{-4}$ (**a**) and 1.23×10^{-3} (**b**) with the Kruskal–Wallis test. **c**, **d** Effect of antiplatelet therapy on the concentrations of circulating whole platelet aggregates and platelet-leukocyte aggregates in CAD patients (n = 38 for no therapy, $n = 73$ for SAPT, $n = 96$ for DAPT). $p = 1.30 \times 10^{-3}$ (**c**) and 3.84×10^{-3} (**d**) with the Kruskal–Wallis test. **e**, **f** Effect of antiplatelet therapy on the concentrations of circulating whole platelet aggregates and platelet-leukocyte aggregates in CAD patients who did not receive anticoagulant therapy ($n = 28$ for no therapy, $n = 58$ for SAPT, $n = 89$ for DAPT). $p = 3.09 \times 10^{-4}$ (**e**) and 9.16×10^{-4} (**f**) with the Kruskal–Wallis test. IQR interquartile range, SAPT single antiplatelet therapy, DAPT dual antiplatelet therapy. Source data are provided as a Source Data file.

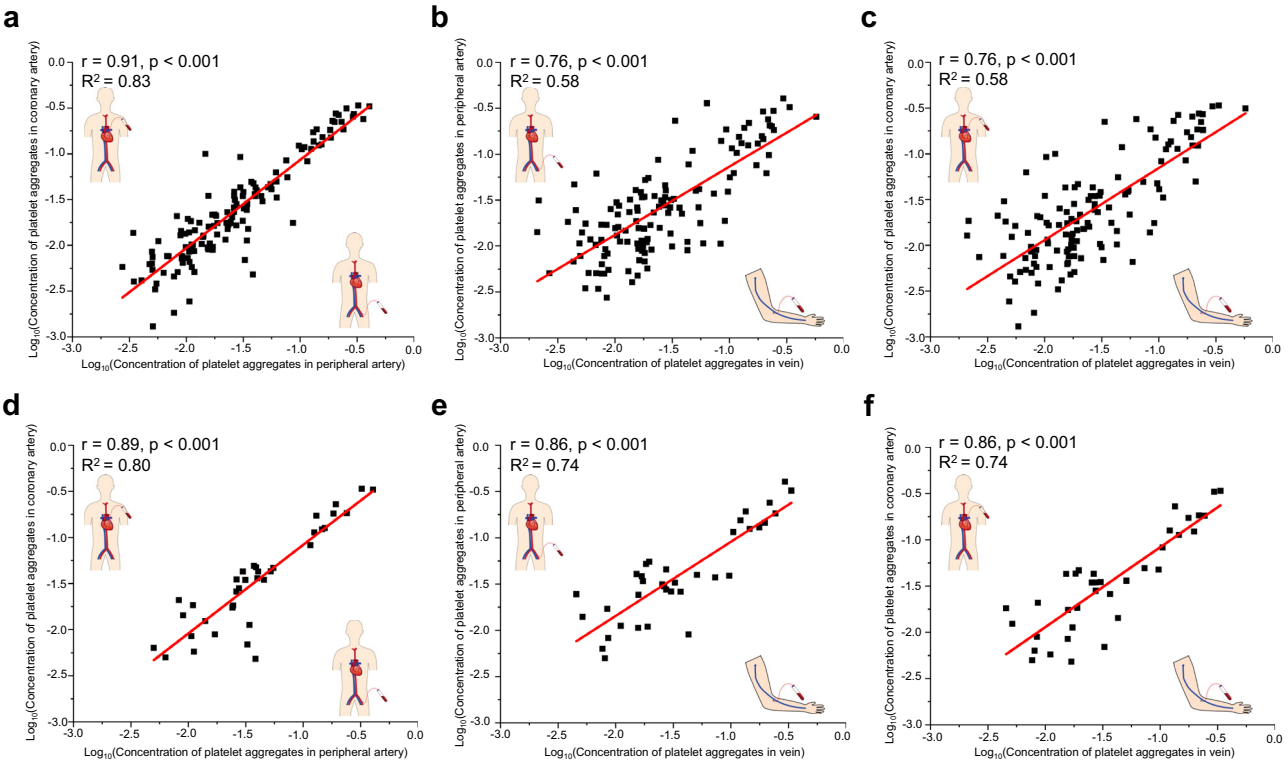

Fig. 5 | Comparison of in vivo platelet aggregation levels across different blood sampling sites in CAD patients. **a**–**c** Associations between the concentrations of circulating whole platelet aggregates in the peripheral artery, coronary artery, and vein in CAD patients ($n = 129$). **d**–**f** Associations between the concentrations of circulating whole platelet aggregates in the peripheral artery, coronary artery, and vein in CAD patients ($n = 36$) on the day of catheterization. *P* values were obtained using the one-sided F test and are shown in the figure. Source data are provided as a Source Data file.

of platelet aggregation in CAD, accurately assessing it has remained technically challenging. In previous research, Satoh et al. observed an increase in circulating platelet aggregate concentration in myocardial infarction patients using an imaging flow cytometer[34]. Michaelson et al. also identified an enhanced concentration of circulating platelet-monocyte aggregates in patients with acute myocardial infarction using a flow cytometer[30]. However, there was a notable lack of comprehensive data on circulating platelet aggregates in broader CAD conditions, such as ACS and CCS. Our study aimed to address this gap by demonstrating that CAD patients, regardless of their use of antiplatelet drugs, exhibit significantly greater platelet aggregation, including not only platelet-leukocyte (platelet-monocyte) aggregates but whole platelet aggregates, compared to healthy individuals. Patients with ACS exhibited a higher level of platelet aggregation compared to those with CCS. This observation can be attributed to the distinct pathophysiological mechanisms underlying each condition: ACS is typically characterized by coronary artery thrombosis following plaque instability, rupture, ulceration, or calcified nodules, whereas CCS is primarily associated with coronary artery stenosis due to stable atherosclerotic plaque buildup. Despite these distinct pathophysiological features, no significant differences were observed in whole platelet aggregate concentrations regardless of these features in ACS patients ($p > 0.300$). The increased platelet aggregation observed in peripheral blood samples from ACS patients indicates that systemic platelet activation is particularly pronounced in the context of ACS, suggesting a heightened thrombotic risk in these patients[3]. This finding is particularly relevant considering that traditional methods for diagnosing CAD primarily involve various anatomical and functional tests[35], yet they often lack simple biochemical or hematological markers for effective detection[36,37]. While C-reactive protein levels, a non-specific inflammatory marker, are elevated in CAD patients[37], and myocardial troponin serves as a specific and robust diagnostic tool for ACS[38], the latter has limited utility in diagnosing CCS[36]. In light of these challenges, our findings propose that evaluating the concentration of circulating platelets in peripheral venous blood could serve as an advanced hematological approach to assist in detecting CAD, applicable to both ACS and CCS cases. This approach could potentially fill the existing gap in diagnostic methods, providing a more direct and specific means of assessing the risk and presence of CAD.

This study builds upon and expands the scope of previous small-scale studies[39,40] by establishing linear correlations in the concentration of circulating platelet aggregates across vein, peripheral artery,

https://doi.org/10.1038/s41467-025-59664-8

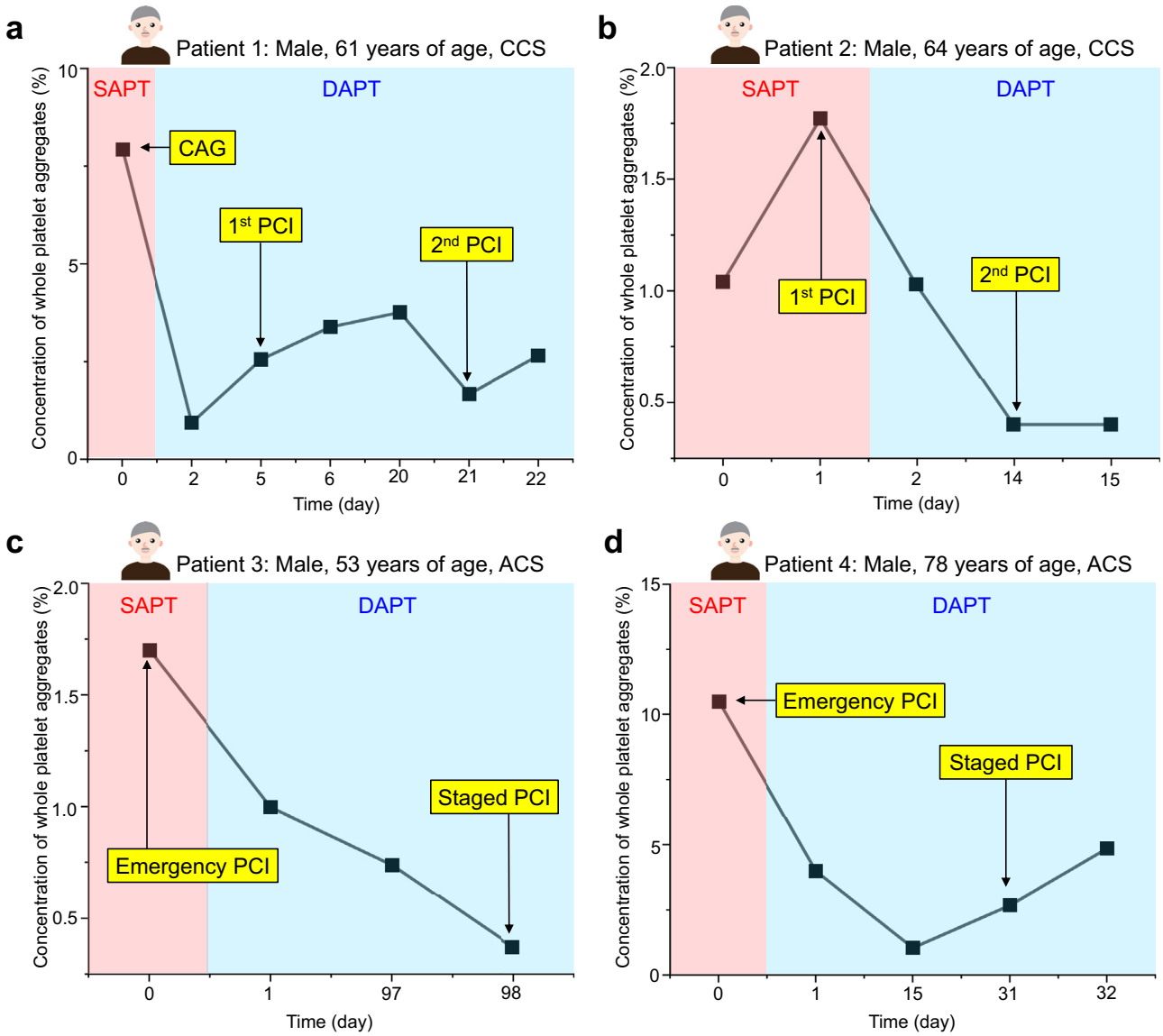

Fig. 6 | Longitudinal assessment of the effect of antiplatelet therapy on in vivo platelet aggregation in CAD patients. a, **b** Patients diagnosed with CCS and treated with SAPT before undergoing PCI procedures. **c**, **d** Patients diagnosed with ACS undergoing an emergency PCI procedure and a staged PCI procedure. ACS acute coronary syndrome, CCS chronic coronary syndrome, SAPT single antiplatelet therapy, DAPT dual antiplatelet therapy, PCI percutaneous coronary intervention. Source data are provided as a Source Data file.

and coronary artery samples. Using the FDM microscope and intelligent phenotypic classification, we were able to rapidly and accurately analyze the size distribution and morphological characteristics of circulating platelet aggregates within extensive imaging datasets. Our findings are in good agreement with a smaller study using flow cytometry on cardiac surgery patients, which found most platelet functional parameters to be consistent between venous and arterial blood, aside from a higher presence of monocyte-platelet and neutrophil-platelet conjugates in venous samples[40]. Similarly, another investigation reported comparable platelet aggregation responses to adenosine diphosphate or arachidonic acid in both types of samples[41], while increased inflammatory cytokines were suggested to contribute to microthrombus formation systemically and locally in both veins and arteries[42]. These corroborating studies partially underpin our observation of strong correlations in whole platelet aggregate concentration and moderate associations in platelet-leukocyte aggregate concentration between venous and arterial samples. Notably, the correlation between circulating whole platelet aggregates and platelet-leukocyte aggregates was more pronounced with same-day blood collection, hinting at the feasibility of using venous samples to estimate real-time platelet aggregation in systemic and coronary arteries. Consequently, our findings advocate for the use of venous blood assessments as a means to gain insights into the dynamics of platelet aggregation across both peripheral and coronary arteries. This approach could significantly streamline the monitoring of platelet aggregation, facilitating the delicate balance between the efficacy of antiplatelet therapy and the risk of bleeding, thereby enhancing patient care in cardiovascular disease management.

This study's single-center, retrospective, and observational nature may limit the generalizability of our findings. Variations in patient characteristics, such as age, sex, and comorbidities, could also influence the observed increase in the concentration of circulating platelet aggregates in CAD patients compared to the control group. Furthermore, due to the cross-sectional design of our study, we could not directly establish a causal link between the concentration of circulating platelet aggregates and specific thrombotic or bleeding events. To truly understand whether an increased concentration of circulating platelet aggregates is predictive of adverse clinical outcomes in the

long term, longitudinal studies are necessary. Such studies would help confirm the potential of circulating platelet aggregates as a biomarker for thrombotic risks and the efficacy of antiplatelet therapy in a more diverse and larger population.

Methods

Human subjects

We retrospectively enrolled 282 patients who underwent CAG or PCI at the University of Tokyo Hospital between October 2022 and December 2023. CAD was defined with significant (≥70%) or intermediate (40–69%) stenosis in CAG[43]. CCS and ACS were defined in accordance with the recently published guidelines[35,44]. After excluding duplicates ($n = 36$), patients without CAD ($n = 17$), and those lacking venous blood samples available for analyses ($n = 22$), the final study population included 207 patients with CAD. The control group comprised 12 healthy participants (6 males, 6 females, ages 23–53). Informed consent for participation in the study was obtained from the patients using an opt-out process on the webpage of the University of Tokyo Hospital. Individuals who refused participation in our study were excluded. Written informed consent was obtained from the healthy participants. The study was conducted in accordance with the Declaration of Helsinki, and the institutional ethics committee of the University of Tokyo approved the study protocol (no. 11049, no. 11344). The subjects were not paid for their participation in this study.

Patient demographics and laboratory parameters

Patient demographic and medical history data were sourced from electronic health records. Peripheral venous blood samples were collected within two weeks prior to the catheterization procedure. We conducted comprehensive laboratory analyses measuring various parameters, including blood cell count, creatinine, low-density lipoprotein (LDL), C-reactive protein (CRP), creatine kinase (CK), B-type natriuretic peptide (BNP), hemoglobin A1c, prothrombin time international normalized ratio (PT-INR), and activated partial thromboplastin time (APTT). Additionally, the estimated glomerular filtration rate (eGFR) was calculated using the abbreviated Modification of Diet in Renal Disease (MDRD) formula: $\mathrm{eGFR}\ (\mathrm{ml/min/1.73\ m^2}) = 194 \times (\mathrm{serum\ creatinine})^{-1.094} \times (\mathrm{age})^{-0.287} \times (0.739\ \text{if female})$. For the assessment of platelets, we used residual coagulation test samples containing 3.2% citrate after the completion of requested clinical laboratory tests at the University of Tokyo Hospital. Similarly, we collected blood samples with 3.2% citrate from one of the 12 healthy subjects on each of 128 different days as the control samples for comparison.

Catheter intervention procedure

The catheter intervention was executed following standard procedures[43]. Initially, a sheath ranging from 5 to 8 Fr was inserted into the radial or femoral artery. Once in place, the activated coagulation time (ACT) was measured, and the residual coagulation test sample was retained for subsequent platelet aggregation analysis. Heparin was then administered at a dose of 3000 U for CAG or 100 U/kg for PCI. Following this, a guiding catheter was engaged in the coronary artery using a 0.035-inch guidewire through the sheath, and ACT was reassessed using the remaining blood sample for further platelet aggregation assessment. In instances of notable stenosis, a functional assessment was conducted, with revascularization performed as deemed necessary by the operator. The PCI was carried out in alignment with established guidelines, encompassing procedures such as balloon dilatation, stent implantation, and atherectomy for calcified lesions[43]. Patients who were free of DAPT before PCI received a loading dose of an antiplatelet drug (mainly the P2Y12 inhibitor) before or during the procedure.

Timing of blood sampling

Preprocedural venous blood samples were drawn within 2 weeks prior to catheterization. During the procedure of CAG or PCI, peripheral arterial samples were derived immediately after inserting a sheath, while coronary arterial samples were obtained through a guiding catheter immediately after the engagement of the catheter. In addition, postprocedural venous sampling was conducted 1–3 days after the procedure. The sampling protocol was applied to multiple procedures in the enrolled patients during the study period.

Sample preparation

Our sample preparation protocol is shown in Supplementary Fig. 1. To enhance the detection efficiency of circulating single platelets and platelet aggregates from whole blood, we employed a density-gradient centrifugation technique as outlined in prior reports[24,29]. In summary, 1 mL of blood, diluted in 5 mL of 0.9% NaCl saline, was layered over Lymphoprep solution (STEMCELLS, ST07851). This mixture was then centrifuged at $800 \times g$ for 20 min following the manufacturer's recommended protocol. After centrifugation, 500 µL of the fluid was extracted from the mononuclear layer. To ensure comprehensive detection of all platelets and platelet aggregates within the sample, platelets were immunofluorescently tagged using 10 µL of anti-CD61-PE (Beckman Coulter, IM3605) and 5 µL of anti-CD45-PC7 (Beckman Coulter, IM3548). To prevent the platelet aggregates from fragmenting due to prolonged storage or shear stress, we added 500 µL of 2% paraformaldehyde (Wako, 163-20145) to the sample, a step that was always completed within 4 h of drawing the blood. Negative control image data were also obtained from healthy subjects under the same sample preparation and image acquisition conditions on the same day to mitigate potential bias in the image data that may have come from experimental variations in blood draw, sample preparation, optical alignment, and hydrodynamic focusing conditions and hence to maintain the state of platelet aggregation in vivo while minimizing the effect of aggregation in vitro.

FDM microscope

The FDM microscope, an advanced high-speed, blur-free, bright-field imaging system, employs a spatially distributed optical frequency comb as its light source and a single-pixel photodetector for image sensing[25,45]. The optical frequency comb, comprising multiple spatially distributed beams, can simultaneously capture the one-dimensional spatial profile of fast-flowing objects such as single platelets and platelet aggregates. Each beam within the comb is uniquely identified by a different modulation frequency, allowing the construction of a spatially encoded image through Fourier transformation of the time-domain waveform captured by the single-pixel photodetector. As detailed in Supplementary Fig. 2a, our setup includes a continuous-wave laser (Cobolt Calypso, 491 nm, 106 mW) as the light source. The laser light undergoes splitting, deflection, and frequency shifting through a series of optical elements, including a beam splitter and acousto-optic deflectors (Brimrose TED-150-100-488, 100-MHz bandwidth), before being recombined and focused onto the flowing objects in a custom hydrodynamic-focusing microfluidic channel (Hamamatsu Photonics) by an objective lens (Olympus UPLSAPO20X, NA:0.75). The transmitted light is then collected by an avalanche photodiode (Thorlabs APD430A/M) and processed using a custom LabVIEW program (LabVIEW 2016) to reconstruct the bright-field images. This FDM microscope boasts a line scan rate of 3 MHz, a spatial resolution of 0.8 µm, a field of view of 53.6 µm × 53.6 µm, and an image resolution of 67 × 67 pixels after correcting the pixel aspect ratio. Additionally, we collected fluorescence emitted from platelets and leukocytes, tagged by anti-CD61-PE and anti-CD45-PC7, respectively, to aid in triggering image acquisitions and identifying platelet aggregates containing leukocytes. The image acquisition operates at an event rate of 100–300 eps, with an event defined as the detection of a single platelet or platelet aggregate. This rate is carefully chosen to prevent microchannel clogging, although the microscope's theoretical event rate exceeds 10,000 eps.

Statistical analysis

Continuous variables were presented as mean ± standard deviations or medians (interquartile ranges) and analyzed using the Kruskal-Wallis test, supplemented by Steel-Dwass posttest corrections. Categorical variables were expressed in counts and percentages. Initially, we evaluated the difference in the concentration of whole platelet aggregates and platelet-leukocyte aggregates between the CAD patient group and healthy individuals. Subsequently, we examined how platelet aggregate concentrations varied with different antithrombotic and antiplatelet therapies. Due to the small number of patients undergoing triple antithrombotic therapy ($n = 7$), we grouped the participants based on the number of antithrombotic drugs they received (0, 1, or ≥ 2). Additionally, a sensitivity analysis was conducted to mitigate the influence of anticoagulant therapy. Furthermore, we explored the relationship between platelet aggregate concentrations across various blood sampling sites using the one-sided F test and linear regression analysis, applying a log transformation to the platelet aggregate concentrations. A p-value of less than 0.05 was deemed indicative of statistical significance. All statistical procedures were carried out using JMP Pro 17 (SAS Institute, Cary, NC) and OriginPro 2023b (OriginLab Corporation, Northampton, MA).

CNN model

AIDeveloper (v. 0.2.3)[26,27], software designed for deep neural network training, was employed to train a CNN model to differentiate images containing noise, platelets, platelet-platelet aggregates, and platelet-leukocyte aggregates (Supplementary Fig. 3a and b). We manually labelled 37,199 images of noise, 66,611 images of single platelets, 12,269 images of platelet aggregates, and 10,274 images of leukocytes using YouLabel (version 0.2.4) to train the CNN model, with 19.4% of the entire dataset designated as the validation set. To create a balanced dataset, random sampling was used. Image augmentation techniques such as rotation, flipping, shifts, brightness adjustments, Gaussian noise, and blur were applied to prevent overfitting. A CNN architecture featuring four convolutional layers and 475,362 trainable parameters was chosen. The CNN structure consists of two sets of convolutional layers with 3x3 kernels and ReLU activation functions, followed by max pooling and dropout (0.25) layers (Supplementary Fig. 3a). Specifically, the first two convolutional layers have 32 filters, and the subsequent two have 64 filters. After flattening the output, a dense layer with 256 units and ReLU activation was used, followed by a dropout of 0.5. The final output layer uses a softmax activation function for classification. A learning rate of 0.0002 was used and the mini-batch size was 128. AIDeveloper (v. 0.2.3) automatically saved the best-performing models based on validation accuracy or loss during the training process. The limited imaging capabilities of the FDM microscope on the microfluidic chip, such as a spatial resolution of only 0.8 µm which is inadequate to clearly resolve platelets measuring 2–3 µm in diameter, the use of two-dimensional imaging for three-dimensional objects, and image blurring caused by imprecise hydrodynamic focusing of cells, resulted in the CNN model achieving an accuracy of 96.4% (Supplementary Fig. 3c, d; Supplementary Fig. 5). This occasionally caused the model to incorrectly identify platelet-related objects and other objects of similar size, leading to erroneous counts of circulating whole platelet aggregates and platelet-leukocyte aggregates (Supplementary Fig. 6). Nevertheless, this did not impact the statistical outcomes presented in Figs. 2–4, as the error rate was below 5%. Also, the errors were uniformly distributed across all classes so there was no significant influence on the overall trends or findings in this work.

Reporting summary

Further information on research design is available in the Nature Portfolio Reporting Summary linked to this article.

Data availability

The authors declare that all data supporting the findings of this study are available within the paper and its Supplementary Information. Other supporting data are available from the corresponding authors upon request. Source data are provided with this paper.

Code availability

All the codes used in this study are available on the Zenodo database with access code 13896279 and from the corresponding authors upon reasonable request.

References

1. Tsao, C. W. et al. Heart disease and stroke statistics-2022 update: a report from the American Heart Association. *Circulation* **145**, e153–e639 (2022).
2. Larsen, S. B. et al. The influence of low-grade inflammation on platelets in patients with stable coronary artery disease. *Thromb. Haemost.* **114**, 519–529 (2015).
3. Heloire, F., Weill, B., Weber, S. & Batteux, F. Aggregates of endothelial microparticles and platelets circulate in peripheral blood. Variations during stable coronary disease and acute myocardial infarction. *Thromb. Res.* **110**, 173–180 (2003).
4. Virmani, R., Kolodgie, F. D., Burke, A. P., Farb, A. & Schwartz, S. M. Lessons from sudden coronary death: a comprehensive morphological classification scheme for atherosclerotic lesions. *Arterioscler. Thromb. Vasc. Biol.* **20**, 1262–1275 (2000).
5. Fuster, V., Badimon, L., Badimon, J. J. & Chesebro, J. H. The pathogenesis of coronary artery disease and the acute coronary syndromes (1). *N. Engl. J. Med.* **326**, 242–250 (1992).
6. Davies, M. J., Bland, J. M., Hangartner, J. R., Angelini, A. & Thomas, A. C. Factors influencing the presence or absence of acute coronary artery thrombi in sudden ischaemic death. *Eur. Heart J.* **10**, 203–208 (1989).
7. Sidney, S. et al. Association between aging of the US population and heart disease mortality from 2011 to 2017. *JAMA Cardiol.* **4**, 1280–1286 (2019).
8. Krumholz, H. M., Normand, S. T. & Wang, Y. Twenty-year trends in outcomes for older adults with acute myocardial infarction in the United States. *JAMA Netw Open* **2**, e191938 (2019).
9. Xaplanteris, P. et al. Five-year outcomes with PCI guided by fractional flow reserve. *N. Engl. J. Med.* **379**, 250–259 (2018).
10. Levine, G. N. et al. Expert consensus document: World Heart Federation expert consensus statement on antiplatelet therapy in East Asian patients with ACS or undergoing PCI. *Nat. Rev. Cardiol.* **11**, 597–606 (2014).
11. Torii, S. et al. Drug-eluting coronary stents: insights from preclinical and pathology studies. *Nat. Rev. Cardiol* **17**, 37–51 (2020).
12. Capodanno, D. et al. Bleeding avoidance strategies in percutaneous coronary intervention. *Nat. Rev. Cardiol.* **19**, 117–132 (2022).
13. Costa, F. et al. Dual antiplatelet therapy duration after percutaneous coronary intervention in high bleeding risk: a meta-analysis of randomized trials. *Eur. Heart J.* **44**, 954–968 (2023).
14. Costa, F. et al. Dual antiplatelet therapy duration based on ischemic and bleeding risks after coronary stenting. *J. Am. Coll. Cardiol.* **73**, 741–754 (2019).
15. Sibbing, D. et al. Updated expert consensus statement on platelet function and genetic testing for guiding P2Y(12) receptor inhibitor treatment in percutaneous coronary intervention. *JACC Cardiovasc. Interv.* **12**, 1521–1537 (2019).
16. Aradi, D. et al. Expert position paper on the role of platelet function testing in patients undergoing percutaneous coronary intervention. *Eur Heart J.* **35**, 209–215 (2014).
17. Price, M. J. et al. Standard- vs high-dose clopidogrel based on platelet function testing after percutaneous coronary intervention: the GRAVITAS randomized trial. *JAMA* **305**, 1097–1105 (2011).
18. Michelson, A. D. Methods for the measurement of platelet function. *Am. J. Cardiol.* **103**, 20A–26A (2009).

19. van der Meijden, P. E. J. & Heemskerk, J. W. M. Platelet biology and functions: new concepts and clinical perspectives. *Nat. Rev. Cardiol* **16**, 166–179 (2019).
20. Tyagi, T. et al. A guide to molecular and functional investigations of platelets to bridge basic and clinical sciences. *Nat. Cardiovasc. Res.* **1**, 223–237 (2022).
21. Zheng, Y. Y. et al. Personalized antiplatelet therapy guided by a novel detection of platelet aggregation function in stable coronary artery disease patients undergoing percutaneous coronary intervention: a randomized controlled clinical trial. *Eur. Heart J. Cardiovasc. Pharmacother.* **6**, 211–221 (2020).
22. Capodanno, D. et al. Dual-pathway inhibition for secondary and tertiary antithrombotic prevention in cardiovascular disease. *Nat. Rev. Cardiol.* **17**, 242–257 (2020).
23. Koupenova, M., Clancy, L., Corkrey, H. A. & Freedman, J. E. Circulating platelets as mediators of immunity, inflammation, and thrombosis. *Circ Res.* **122**, 337–351 (2018).
24. Nishikawa, M. et al. Massive image-based single-cell profiling reveals high levels of circulating platelet aggregates in patients with COVID-19. *Nat. Commun.* **12**, 7135 (2021).
25. Nitta, N. et al. Intelligent image-activated cell sorting. *Cell* **175**, 266–276 e213 (2018).
26. Mikami, H. et al. Ultrafast confocal fluorescence microscopy beyond the fluorescence lifetime limit. *Optica* **5**, 117–126 (2018).
27. Krater, M. et al. AIDeveloper: deep learning image classification in life science and beyond. *Adv. Sci.* **8**, e2003743 (2021).
28. Bradski, G. The opencv library. *Dr Dobb's J Softw Tools Prof Program.* **25**, 120–126 (2000).
29. Zhang, C. et al. Real-time intelligent classification of COVID-19 and thrombosis via massive image-based analysis of platelet aggregates. *Cytometry A* **103**, 492–499 (2023).
30. Michelson, A. D., Barnard, M. R., Krueger, L. A., Valeri, C. R. & Furman, M. I. Circulating monocyte-platelet aggregates are a more sensitive marker of in vivo platelet activation than platelet surface P-selectin: studies in baboons, human coronary intervention, and human acute myocardial infarction. *Circulation* **104**, 1533–1537 (2001).
31. Hui, H., Fuller, K. A., Erber, W. N. & Linden, M. D. Imaging flow cytometry in the assessment of leukocyte-platelet aggregates. *Methods* **112**, 46–54 (2017).
32. Linden, M. D. et al. Indices of platelet activation and the stability of coronary artery disease. *J Thromb Haemost* **5**, 761–765 (2007).
33. Zhou, Y. et al. Long-term effects of Pfizer-BioNTech COVID-19 vaccinations on platelets. *Cytometry A* **103**, 162–167 (2023).
34. Satoh, K. et al. Clear visual detection of circulating platelet aggregates in acute myocardial infarction using a flow cytometer equipped with an imaging device. *Platelets* **15**, 61–62 (2004).
35. Knuuti, J. et al. 2019 ESC Guidelines for the diagnosis and management of chronic coronary syndromes. *Eur. Heart J.* **41**, 407–477 (2020).
36. Laufer, E. M. et al. The extent of coronary atherosclerosis is associated with increasing circulating levels of high sensitive cardiac troponin T. *Arterioscler Thromb Vasc. Biol.* **30**, 1269–1275 (2010).
37. Danesh, J. et al. C-reactive protein and other circulating markers of inflammation in the prediction of coronary heart disease. *N. Engl. J. Med.* **350**, 1387–1397 (2004).
38. Keller, T. et al. Sensitive troponin I assay in early diagnosis of acute myocardial infarction. *N. Engl. J. Med.* **361**, 868–877 (2009).
39. Spiezia, L. et al. On-treatment platelet reactivity in peripheral and coronary blood in patients undergoing primary PCI for ST-segment elevation myocardial infarction (STEMI). *Scand. J. Clin. Lab Investig.* **78**, 281–286 (2018).
40. Tornudd, M. et al. Quantification of platelet function - a comparative study of venous and arterial blood using a novel flow cytometry protocol. *Platelets* **33**, 926–934 (2022).
41. Kafian, S., Mobarrez, F., Kalani, M., Wallen, H. & Samad, B. A. Comparison of venous and arterial blood sampling for the assessment of platelet aggregation with whole blood impedance aggregometry. *Scand. J. Clin. Lab. Investig.* **71**, 637–640 (2011).
42. Nishimura, S. et al. In vivo imaging visualizes discoid platelet aggregations without endothelium disruption and implicates contribution of inflammatory cytokine and integrin signaling. *Blood* **119**, e45–e56 (2012).
43. Lawton, J. S. et al. 2021 ACC/AHA/SCAI guideline for coronary artery revascularization: a report of the American College of Cardiology/American Heart Association Joint Committee on Clinical Practice Guidelines. *Circulation* **145**, e18–e114 (2022).
44. Byrne, R. A. et al. 2023 ESC Guidelines for the management of acute coronary syndromes. *Eur. Heart J.* **44**, 3720–3826 (2023).
45. Vaidyanathan, R., Yeo, T. & Lim, C. T. Microfluidics for cell sorting and single cell analysis from whole blood. *Methods Cell Biol* **147**, 151–173 (2018).

Acknowledgements

This work was supported by AMED JP23hma922009 (M.N., N.N., S.K., K.G.) and JP20wm0325021 (M.N., K.G., Y.Y.), JSPS KAKENHI grant numbers 19H05633 (K.G.), 20H00317 (K.G.), JP21K15640 (M.N.), JP23H02810 (M.N., K.G.), JSPS Core-to-Core Program JPJSCCA20190007 (K.G.), UTOPIA Research Grants for Young Researchers JP223fa627001 (Y.Z.), White Rock Foundation (K.G.), Nakatani Foundation (K.G.), Charitable Trust Laboratory Medicine Research Foundation of Japan (M.N.), and KAKETSUKEN (K.G., M.N., Y.Y.). We acknowledge support from Serendipity Lab. We thank Enas Elkhateeb, Yoshika Kusumoto, and Kaori Ono for their assistance with the sample preparation.

Author contributions

K.H., S.K., M.N., and K.G. conceived and designed the work. K.H., S.K., M.N., M.S., Y.Z., H.Z., S.M., J.I., Nf.T., H.W., C.K., Y.D., J.C., C.Z., J.A., and R.Y. contributed to the acquisition and analysis of the data. M.N., Y.Z., H.W., Y.D., J.C., C.Z., and J.A. prepared the blood samples. Y.I. and H.K. designed and constructed the FDM microscope. Y.Z., H.Z., N.N., T.S., and K.G. developed the software to analyze the data. H.Z., H.W., C.K., Y.D., J.C., C.Z., J.A., Y.I., and R.Y. performed the image acquisition. K.H., S.K., M.N., Y.Z., H.Z., S.M., J.I., Nf.T., N.N., M.K., Y.Y., and K.G. interpreted the data. K.H. and K.G. drafted the manuscript. All authors critically revised the manuscript. All authors provided final approval and agreed to be accountable for all aspects of the work, ensuring integrity and accuracy. M.N., N.N., and K.G. acquired funding for the work. Nh.T., M.K., Y.Y., and K.G. supervised the work.

Competing interests

N.N., T.S., and K.G. are shareholders of CYBO, which is a company developing cell analysis technology and using artificial intelligence to process cells. The other authors declare no other competing interests.

Additional information

Supplementary information The online version contains supplementary material available at https://doi.org/10.1038/s41467-025-59664-8.

Correspondence and requests for materials should be addressed to Masako Nishikawa or Keisuke Goda.

Peer review information *Nature Communications* thanks Richard Becker, Jun Ding, and the other, anonymous, reviewer(s) for their contribution to the peer review of this work. A peer review file is available.